HHS Public Access

Author manuscript

Mol Cell. Author manuscript; available in PMC 2015 April 01.

Published in final edited form as:

Mol Cell. 2003 November ; 12(5): 1251–1260.

Direct Binding of the PDZ Domain of Dishevelled to a Conserved Internal Sequence in the C-Terminal Region of Frizzled

Hing-C. Wong[1], **Audrey Bourdelas**[3], **Anke Krauss**[5], **Ho-Jin Lee**[1], **Youming Shao**[1], **Dianqing Wu**[4], **Marek Mlodzik**[5], **De-Li Shi**[3,*], and **Jie Zheng**[1,2,*]

[1]Department of Structural Biology, St. Jude Children's Research Hospital, Memphis, Tennessee 38105

[2]Department of Molecular Sciences, University of Tennessee Health Science Center, Memphis, Tennessee 38163

[3]Laboratoire de Biologie du Dévelopment, CNRS UMR 7622, University Pierre et Marie Curie, 9 quai Saint-Bernard, 75005 Paris, France

[4]Department of Genetics and Development Biology, University of Connecticut Health Center, Farmington, Connecticut 06030

[5]Brookdale Department of Molecular, Cell and Developmental Biology, Mt. Sinai School of Medicine, New York, New York 10029

Summary

The cytoplasmic protein Dishevelled (Dvl) and the associated membrane-bound receptor Frizzled (Fz) are essential in canonical and noncanonical Wnt signaling pathways. However, the molecular mechanisms underlying this signaling are not well understood. By using NMR spectroscopy, we determined that an internal sequence of Fz binds to the conventional peptide binding site in the PDZ domain of Dvl; this type of site typically binds to C-terminal binding motifs. The C-terminal region of the Dvl inhibitor Dapper (Dpr) and Frodo bound to the same site. In *Xenopus*, Dvl binding peptides of Fz and Dpr/Frodo inhibited canonical Wnt signaling and blocked Wnt-induced secondary axis formation in a dose-dependent manner, but did not block noncanonical Wnt signaling mediated by the DEP domain. Together, our results identify a missing molecular connection within the Wnt pathway. Differences in the binding affinity of the Dvl PDZ domain and its binding partners may be important in regulating signal transduction by Dvl.

Introduction

Wnt signaling pathways are essential for development (Cadigan and Nusse, 1997; Moon et al., 2002) and have been implicated in tumorigenesis (Taipale and Beachy, 2001). Of the distinct Wnt pathways, the canonical Wnt signaling pathway, which involves the inhibition of GSK3β activity and stabilization of β-catenin in the cytoplasm, is essential for the

*Correspondence: jie.zheng@stjude.org (J.Z.), dsh@iccr.jussieu.fr (D.-L.S.).

Accession Numbers: The atomic coordinates have been deposited under accession code 1MC7 in the Protein Data Bank.

specification of cell fate in *Drosophila* and *Xenopus*. The noncanonical Wnt pathway, which involves the Rho family of GTPases and JNK, affects planar polarity in the same species (Moon and Shah, 2002). The Wnt/Calcium pathway stimulates intracellular calcium release in a G protein-dependent manner (Kühl et al., 2000). In all these pathways, the 7 transmembrane domain Fz proteins are bound by the secreted molecule Wnt and transduce the signal to the cytoplasmic protein Dvl (Siegfried et al., 1994; Noordermeer et al., 1994; Krasnow et al., 1995; Shulman et al., 1998), the component at which these signaling pathways diverge (Axelrod et al., 1998; Boutros et al., 1998; Li et al., 1999). Dvl also functions in a feedback loop of Fz (Tree et al., 2002). However, a direct interaction between Fz and Dvl has not been shown, and the mechanism by which Dvl distinguishes between different Wnt pathways has not been defined (Wharton, 2003).

Dvl proteins are composed of an N-terminal DIX domain, a central PDZ domain, and a C-terminal DEP domain (Wong et al., 2000). Of these three, the PDZ domain appears to play an important role in both the canonical and noncanonical Wnt pathways (Moon and Shah, 2002). In addition, several molecules can interact with the PDZ domain (Yan et al., 2001; Rousset et al., 2001; Gloy et al., 2002; Park and Moon, 2002; Cheyette et al., 2002). Indeed, it has been suggested that the PDZ domain of Dvl is involved in distinguishing between the two pathways (Boutros and Mlodzik, 1999; Weston and Davis, 2001). To test such an hypothesis, we investigated the interactions between the PDZ domain (residues 247-341) of mouse Dvl1 (mDvl1) and its binding partners by using nuclear magnetic resonance (NMR) spectroscopy. We discovered that the same peptide-interacting site of the mDvl1 PDZ domain interacts with different molecules whose sequences have no obvious homology. One peptide that binds to the mDvl1 PDZ domain is the conserved motif (KTXXXW) of Fz, which is located two amino acids after the seventh transmembrane domain (Umbhauer et al., 2000), although it is not a typical PDZ binding motif (Hung and Sheng, 2002; Cowburn, 1997). This finding revealed a previously unknown connection between the membrane-bound receptor and downstream components of the Wnt signaling pathways. On the basis of these studies, we have conducted further analyses of the function(s) of Dvl to distinguish different signals in a complex cellular network of signal transduction.

Results and Discussion

Solution Structure of the PDZ Domain of mDvl1

To examine the interactions between the PDZ domain of mDvl and its binding partners, we first determined the solution structure of the PDZ domain. The structure was elucidated on the basis of 1124 NMR-derived constraints. Twenty structures that best fit the experimental constraints in the structural calculation were analyzed. The structure resembles that of the typical PDZ-domain fold. Unlike class I PDZ domains (Bezprozvanny and Maximov, 2001; Hung and Sheng, 2002), the mDvl1 PDZ domain lacks the conserved His at a G-H (glycine and histidine) position in the peptide binding pocket (Figure 1). Moreover, the mDvl1 PDZ domain differs from class II PDZ domains in that it has no hydrophobic residues at its G-H positions (Daniels et al., 1998) (Figure 1).

High Specificity of the Molecular Recognition of the Dvl PDZ Domain

We next analyzed the interactions between the PDZ domain and several binding partners by conducting chemical-shift perturbation NMR spectroscopy as described by Wuthrich (2000). The method can be used to precisely map binding sites and is well suited to detect weak but specific biologically relevant interactions (Zheng et al., 1996; Wong et al., 2002). We first analyzed the interaction between the C-terminal residues of Dpr or Frodo (Cheyette et al., 2002; Gloy et al., 2002) and residues 247 through 341 of the mDvl1 PDZ domain; similar analyses of the *Xenopus* homolog have been done by using X-ray crystallography (Cheyette et al., 2002). We used a peptide comprising the C-terminal 10 residues of Dpr/Frodo (SGSLKLMTTV, designated Dpr/Frodo peptide) to titrate the ^{15}N-labeled PDZ domain of mDvl1 and found that the Dpr/Frodo peptide bound to the peptide binding groove, a result similar that observed in *Xenopus* homolog studies (Cheyette et al., 2002). We then examined the interaction between Van Gogh (an inhibitor of canonical Wnt signaling) and the PDZdomainofmDvl1. Despite a high degree of similarity to the C-terminal region of Dpr/Frodo, the peptide corresponding to the 11 C-terminal residues of Van Gogh (FVMRLQSETSV), when added to the solution of ^{15}N-labeled PDZ domain, caused no chemical-shift perturbation. This result is consistent with the observation that the interaction between Van Gogh and Dvl requires both the Dvl PDZ domain and the basic region that is N-terminal to the PDZ domain and was not present in our construct (Park and Moon, 2002).

Direct Interaction between the Conserved Motif KTXXXW of Fz and the PDZ Domain of Dvl

We investigated the possible interaction between Fz and Dvl. Previous studies have demonstrated that the C-terminal region of Fz transduces the canonical Wnt signal (Umbhauer et al., 2000). Moreover, a conserved motif (KTXXXW) located two amino acids C-terminal to the seventh transmembrane domain is required for activation of the canonical Wnt pathway and for membrane relocalization and phosphorylation of Dvl (Umbhauer et al., 2000). When a synthetic peptide that consisted of Fz7 residues 525 through 536 (G**KT**LQS**W**RRFYH, designated the Fz7 peptide) was added to the solution of the ^{15}N-labeled PDZ domain, we observed a chemical-shift perturbation similar to that seen when the Dpr/Frodo peptide was added to the same type of solution.

Examination of a series of ^{1}H-^{15}N correlation spectra for the ^{15}N-labeled mDvl1 PDZ domain (Figure 2A) revealed that the Fz7 peptide, although an internal sequence, bound to the conventional C-terminal peptide-binding groove (Cowburn, 1997) located between αB and βB (Figures 2B and 2C). Binding was essentially abolished when three conserved amino acids in the Fz7 peptide were mutated (replacements in boldface type: G**MV**LQS**G**RRFYH, designated mutFz7). Furthermore, two single-mutation peptides, G**M**TLQSWRRFYH, designated Fz7K/M, and GKTLQS**G**RRFYH, designated Fz7W/G, bound to the PDZ domain with an affinity that was much weaker than that of the Fz7 peptide. These results demonstrated that the three residues in Fz are essential to binding to Dvl and that the C terminus of the Fz7 peptide does not bind to the PDZ domain. Although internal peptides rarely bind to PDZ domains, an internal sequence within a context of β-hairpin conformation has been shown to compete with a conventional C-terminal motif that binds to PDZ domains (Hillier et al., 1999; Tochio et al., 2000). Nevertheless, the Fz-Dvl interaction that we identified is an example of an internal sequence of an otherwise unstructured receptor

cytoplasmic tail that can interact with a PDZ domain. Moreover, it is unusual that both the internal sequence and C-terminal peptides can bind to the same binding site on the PDZ domain.

Binding of the Fz C Terminus to Dvl PDZ Domain In Vitro

To further characterize the binding properties of the C terminus of Frizzled proteins, we performed a yeast two-hybrid screen with the C-terminal domain of *Drosophila* Fz2 as bait. By screening a library of 10^6 clones, we isolated 6 clones that encoded *Drosophila* Dishevelled (Dsh). Using the same two-hybrid assay, we confirmed that the C terminus of Fz2 and of Fz can bind to Dsh. Such binding was not affected by the deletion of the last five amino acids of either Fz or Fz2 (Table 1). This finding is consistent with our previous observation that the C termini of Frizzled proteins bind to Dvl/Dsh through an internal sequence motif.

To further demonstrate that the Fz7 peptide interacts with the mDvl1 PDZ domain, we conducted biotin pulldown assays. The N termini of both the Fz7 peptide and the Dpr/Frodo peptide were biotinylated, and after biotinylation the peptides were coupled to agarose beads immobilized with avidin. The Fz7- and Dpr/Frodo-coupled beads bound to the purified PDZ domain (Figure 3A), and their binding affinities were similar. Furthermore, we found that the PDZ domain bound to Fz7 peptide-coupled beads can be eluted by the Dpr/Frodo peptide. This result indicated that the Fz7 peptide and the Dpr/Frodo peptide compete for the same site on the surface of the PDZ domain. It is consistent with those of the NMR spectroscopy studies.

The binding affinities between the PDZ domain and the Fz7 and Dpr/Frodo peptides were also measured by using fluorescence spectroscopy. The binding of the Dpr/Frodo peptide quenched the intrinsic tryptophan fluorescence of the PDZ domain. By monitoring such changes in fluorescence intensity, we determined that the binding affinity between the Dpr/Frodo peptide and the PDZ domain was 16.1 ± 0.7 μM. However, the tryptophan residue within the Fz7 peptide prevented us from using this method to directly determine the binding affinity between this peptide and the PDZ domain. Nevertheless, we determined that the Fz7 peptide inhibits the binding of the Dpr/Frodo peptide to the PDZ domain in the manner of classical competitive inhibition (Figure 3C). The estimated inhibition constant, K_I, which was equivalent to the mean binding affinity between the Fz7 peptide and the PDZ domain, was 9.5 ± 7.9 μM (K_I values obtained from two independent measurements were 5.9 ± 0.5 μM and 12.8 ± 3.9 μM, Figure 3C). Furthermore, by using the mutated Fz7 peptide Fz7W/G (GKTLQS**G**RRFYH), which does not have an intrinsic tryptophan, we conducted fluorescence spectroscopy analysis of the binding affinity between this mutated peptide and the PDZ domain. The measured affinity was 100 times weaker than that of wild-type (K_d = 1.3 ± 0.4 mM, the mean of two independent measurements).

The well-defined but relatively weak (K_d~10 μM) interaction between the Fz7 peptide and the mDvl1 PDZ domain suggests that other regions of Dvl are required for signal transduction between membrane-bound Fz and Dvl. Although the DEP domain of Dvl does not bind to the Fz7 peptide (data not shown), previous studies have indicated that the DEP domain plays a role in the membrane localization of the protein (Wong et al., 2000; Axelrod

et al., 1998, 2001; Rothbacher et al., 2000; Boutros et al., 1998). Therefore, signal transduction between Fz and Dvl may require the membrane-targeting function of the DEP domain to bring the two proteins into close proximity to one another. Indeed, it may be a common feature that multiple interactions are involved in a specific Dvl reorganization event. Another such example is the interaction between Dpr/Frodo and Dvl. Although deletion of the C-terminal residues of Frodo abolished interaction with Dvl, the DIX domain and adjacent Dvl sequence are also important to the Frodo-Dvl association (Gloy et al., 2002). The C-terminal residues of Dpr/Frodo bind to the Dvl PDZ domain (Cheyette et al., 2002), and, as we showed in this report, the binding affinity is relatively low ($K_d \sim 16\ \mu M$). However, all of these weak but specific interactions orchestrate the association event, and the disruption of any one of these weak interactions may cause the breakdown of binding.

Inhibition of the Canonical Wnt Pathway by Fz7 and Dpr/Frodo Peptides

To further examine the role of the PDZ domain of Dvl in the canonical and noncanonical Wnt signaling pathways, we tested the effects of the PDZ binding peptides on Wnt signaling. Because mutations in the conserved KTXXXW motif of Fz abolish Fz activity in the canonical Wnt signaling pathway (Umbhauer et al., 2000), we coinjected peptides that contained various mutations in the KTXXXW motif and different activators of the canonical Wnt pathway into the animal-pole region of *Xenopus* embryos at the 8 cell stage (Umbhauer et al., 2000). We then performed RT-PCR to analyze expression of the Wnt target gene *Siamois* in ectodermal explants that were dissected from blastulae and cultured until they reached the early gastrula stage. Although the mutFz7 peptide had little effect on *Siamois* expression induced by Wnt1 and Dvl, the Fz7 peptide inhibited *Siamois* expression induced by Wnt1 and Dvl (Figure 4A). In addition, the Fz7 peptide did not block *Siamois* expression induced by dominant-negative GSK3β and by β-catenin, but it reduced *Siamois* expression induced by Xfz3 (Figure 4B); these results indicate that the Fz7 peptide disrupts canonical Wnt signaling at the level of Dishevelled. These results are consistent with the notion that the binding of the internal sequence of Fz to the PDZ domain of Dvl is important for signaling in the canonical Wnt pathway. Furthermore, a separate experiment revealed that Dvl translocates to the membrane of ectodermal cells of *Xenopus* embryos when they are given injections of full-length *Drosophila* Fz mRNA and Dvl mRNA (data not shown). However, coinjections of the C-terminal region of Fz into the ectodermal cells did not cause Dvl to localize to the membrane. Because full-length Fz, but not its C-terminal portion, is membrane bound, these results further indicate the direct interaction between Fz and Dvl.

Fz7 and Dpr/Frodo Peptide-Mediated Inhibition of Wnt1-Induced Secondary Axis Formation

We tested whether the peptides affect the well-known ability of Wnt to induce secondary axis formation. *Wnt1* mRNA injected into the ventro-vegetal region of *Xenopus* embryos at the 4 cell stage induced the formation of a complete secondary axis (Figures 4C and 4D). The peptide with a mutated KTXXXW motif (mutFz7) did not significantly block secondary axis formation (Figure 4E), whereas Fz7 and Dpr/Frodo peptides substantially reduced the extent of secondary axis formation induced by Wnt1 (Table 2). This reduction resulted in embryos with a partial secondary axis or only a single axis (Figures 4F and 4G). Therefore, Fz7 and Dpr/Frodo peptides specifically block signaling in the canonical Wnt pathway.

Furthermore, the blockage of secondary axis formation by Fz7 and Dpr/Frodo peptides did not result from defects in gastrulation because ventral injection of these peptides, either alone or with Wnt1, did not affect gastrulation movements (data not shown). Incomplete blockage of the Wnt signaling by both the Fz7 and Dpr/Frodo peptides is likely due to the relative weak interactions between these peptides and Dvl. Indeed, the result of our coinjection experiments using the Dpr/Frodo peptide is consistent with those of earlier experiments in which *Wnt8* mRNA and a small C-terminal fragment of Frodo (FrdC) were coinjected into *Xenopus* embryos (Gloy et al., 2002). The effect of the Fz7 peptide on canonical Wnt signaling is dose dependent. A higher concentration (200 μM) efficiently blocked Wnt1-induced secondary axis formation, whereas a low concentration (50 μM) had a weak effect (Table 2).

Lack of Interference by the Fz7 Peptide with the DEP-Mediated Noncanonical Wnt Pathway

Although the Fz7 peptide blocks canonical Wnt signaling, it is unclear whether it interferes with other Wnt pathways. The noncanonical Wnt pathway that involves the DEP domain is required for planar cell polarity in *Drosophila* (Axelrod, 2001) and for convergent extension in *Xenopus* (Sokol, 1996). Therefore, we conducted the *Xenopus* explant elongation assay to test whether the Fz7 peptide interferes with this noncanonical pathway. Ectodermal explants that were treated with activin at the blastula stage and cultured until they reached the neurula stage exhibited extensive elongation that mimics convergent extension (Figures 4H and 4I). Gain of function by overexpression of full-length Xfz7 blocked elongation (Djiane et al., 2000) (Figure 4J), and this blockage was rescued by coinjection of the Fz7 peptide and Xfz7 (Figure 4K). This result suggests that the Fz7 peptide disrupts the interaction between the Xfz7 receptor and the PDZ domain of Dvl and is consistent with the requirement of the PDZ and DEP domains in planar cell polarity signaling (Boutros and Mlodzik, 1999). A truncated Dvl protein, i.e., Xdd1 that lacked the PDZ domain, also blocked elongation of the ectodermal ex-plant (Figure 4L) (Sokol, 1996). However, coinjection of the Fz7 peptide did not rescue explant elongation blocked by Xdd1 (Figure 4M). This result implies that the Fz7 peptide does not interfere with the DEP domain of Xdd1 and thus does not affect the noncanonical Wnt pathway. Together, these observations further suggest a specific interaction of the Fz7 peptide with the PDZ domain of Dvl.

Conclusion

We have demonstrated that there is a direct interaction between Fz and Dvl. Specifically, the PDZ domain of mDvl1 interacts directly with the Fz conserved sequence that is C-terminal to the seventh transmembrane helix. This interaction is essential in the transduction of the Wnt signal from Fz to the downstream components of the pathway. Thus, our finding sheds light on the mechanism by which the receptor Fz communicates with the downstream component Dvl. Furthermore, our findings should be useful in designing pharmaceutical antagonists that modulate Wnt signaling in tumor cells.

The interaction between Fz and Dvl is relatively weak; we therefore hypothesize that the membrane-targeting function of the Dvl DEP domain is required to ensure signal transduction. The weak interaction between Fz and Dvl could allow signaling from Fz to be

mediated by cytoplasmic proteins, e.g., Dpr/Frodo. Indeed, the Dvl1 PDZ domain uses a single recognition site to interact with Fz and Dpr/Frodo. In addition, because of the weak interaction, the local physiological condition and the local environment, which includes the local concentrations of Dvl and its regulatory effectors, should play a considerable role in the mediation of the molecular recognition of Dvl (Nooren and Thornton, 2003). This possibility may serve as an explanation for the following discrepancy: despite the 90% amino acid identity between Dpr and Frodo (Wharton, 2003), Dpr negatively regulates Wnt signaling (Cheyette et al., 2002), whereas Frodo enhances Wnt signaling (Gloy et al., 2002).

Multiple homologs of Fz and Dvl are present in mammals. The differences in the sequences of the PDZ domains of Dvl1 homologs (Figure 1) and the C-terminal regions of Fz receptors suggest that the binding affinities of each in the Fz-Dvl complexes should differ. Further studies to fully investigate such differences will provide insight into the signaling pathways that involve Fz and Dvl.

Experimental Procedures

Purification of the mDvl1 PDZ Domain

The cDNA that encodes the mDvl1 PDZ domain (amino acids 247-341) was subcloned into the pET28a vector; the cDNA was inserted so that a region encoding a 6xHis tag was linked to the 5′ of the cDNA. The 6xHis-tagged protein was expressed in BL21(DE3)-RP *E. coli* cells. Site-directed mutagenesis was done to replace particular codons in the cDNA with those commonly used by bacteria. No change in peptide sequence was caused by these codon replacements. To improve the protein solubility and to prevent dimerization, Cys334 was replaced with alanine. No change in the ^{15}N-HSQC spectra after the mutation indicated that the structure of the altered PDZ domain remained the same as that of the wild-type protein.

Transformed cells were grown in MOPS-containing medium with 1 gL^{-1} $^{15}NH_4Cl$ as the source of ^{15}N and 3 gL^{-1} $^{13}C_6$-glucose as the source of ^{13}C. Protein expression was induced by the addition of 1 mM isopropyl-1-thio-β-D-galactoside (IPTG) when the OD_{600} of the cells was approximately 0.7; 6 hr after induction, the cells were resuspended in lysis buffer and sonicated, and the lysate was centrifuged. The supernatant was then transferred to a column of Ni-NTA beads, and the column was washed with 50 mM imidazole. The protein was eluted by 200 mM imidazole in 20 mM phosphate buffer (pH 7.5) and 300 mM NaCl. The PDZ domain was further purified by chromatography using a Superdex 75-pg column (Amersham Pharmacia) and was eluted by 100 mM phosphate buffer (pH 7.5).

NMR Spectroscopy and Structure Calculation

NMR experiments were performed with a Varian INOVA 600 MHz NMR spectrometer at 25°C. Samples consisted of the PDZ domain (0.8–1.5 mM) in 100 mM phosphate buffer (pH 7.5), 10% D_2O, and 0.5 mM EDTA. HNCACB and CBCA(CO)NH were performed to determine the backbone assignment. Side-chain proton and carbon resonances were assigned on the basis of the results of the HCCH-TOCSY and HCCH-COSY experiments.
The $^3J_{HN\text{-}H\alpha}$ coupling constant was measured by J-HMQC.NOE connections were assigned

on the basis of three-dimensional ^{15}N-edited NOESY and ^{13}C-edited NOESY. NMR spectra were processed with NMRpipe (Delaglio et al., 1995) software and analyzed by XEASY (Xia et al., 1993). Integrated NOE peaks were calibrated and converted to distance constraints with the program CALIBA (Guntert et al., 1991). A total of 1124 meaningful distance constraints were derived. In addition, 44 dihedral angle restraints and 20 distance restraints from hydrogen bonds obtained from NMR experiments were added. The program DYANA (Guntert et al., 1997) was used for the final structural calculation. Twenty structures with the lowest target functions were selected from a total of 320 calculated structures (see Supplemental Data at http://www.molecule.org/cgi/content/full/12/5/1251/DC1).

Yeast Two-Hybrid System

For this study, the MATCHMAKER two-hybrid system (Clontech, Inc.) was used. In brief, in the screening experiments, pGBT9 was used as the bait plasmid to express the *Drosophila* Fz2 C terminus fused to the Gal4 DNA binding domain. A *Drosophila* imaginal disc library was used as prey. In the mating assay, the full-length *Drosophila* Dsh clone, which was isolated in the screen, was used as prey; the cytoplasmic C-terminal sequences of Fz and Fz2 and their deletion constructs were used as bait (see Table 1). β-Gal activity was determined by colony-lift filter assays in which X-Gal served as the substrate.

Peptide Synthesis and Purification

Peptides were chemically synthesized by the Hartwell Center for Bioinformatics & Biotechnology at St. Jude Children's Research Hospital. Amino groups were attached to the N terminus of each peptide; carboxylate groups, to the C terminus. Peptides were purified by reverse-phase high-performance liquid chromatography and lyophilized.

Biotin Pull-Down Experiment

UltraLink Immobilized Monomeric Avidin was obtained from Pierce (Pierce Biotechnology, Inc.), and the pull-down experiments were conducted in accordance with a standard protocol provided by the manufacturer. PBS was used as buffer throughout the experiments. In brief, for each pull-down experiment, 100 μl of avidin-conjugated beads were incubated with 200 pmol of biotinylated peptide, either Fz7 or Dpr/Frodo, for 2 hr at room temperature. The peptide-charged beads were then incubated with 25 pmol of purified PDZ domain at 4°C for 2 hr. After the beads were washed at least 5 times with buffer, they underwent SDS-PAGE. When the Dpr/Frodo peptide was used to compete with the Fz7 peptide (lane 6, Figure 3A), the Fz7 peptide-coupled beads that were bound by PDZ were subjected to an additional 5 washes with buffer that contained 0.5 mM Dpr/Frodo peptide.

Fluorescence Spectroscopy

A Jobin-Yvon Fluorolog-3 spectrofluorometer (Jobin-Yvon, Inc.) was used to obtain the fluorescence measurements of the interaction between the PDZ domain of mDvl1 and the Dpr/Frodo peptide. Titration experiments were performed at 10°C in a phosphate buffer (0.1 M potassium phosphate; 0.5 mM EDTA [pH 7.5]). The peptide ligand (2 mM) was injected into the 2.0 ml sample cell that contained either the PDZ domain (10 μM) or the mixture of

the PDZ domain (10 μM) and the Fz7 peptide (10 μM or 50 μM). The excitation wavelength was 290 nm (slit width, 5 nm), and the fluorescence emissions from 320 nm to 370 nm (slit width, 5 nm) were recorded (Figure 3B) during the titration of Dpr/Frodo, whose concentrations ranged from 2 μM to 90 μM. The fluorescence data were analyzed by the ORIGIN program (Microcal). Fitting was performed to extract the maximum fluorescence intensity quenching (F_{max}), the binding affinity of the Dpr/Frodo peptide and the PDZ domain (K_d), and the inhibition constant (K_I) of Fz7 in its disruption of the interaction between the PDZ domain and the Dpr/Frodo peptide. The KI value was calculated from a reciprocal plot of fluorescence intensity quenching (ΔF) against the concentration of the Dpr/Frodo peptide for three sets of titration data.

Xenopus Embryos and Microinjections of mRNA and Peptides

Xenopus eggs were obtained from females that had received injections of 500 IU of human chorionic gonadotropin (Sigma) and had been artificially fertilized. Synthesis and microinjection of capped mRNAs were done as described (Umbhauer et al., 2000). To assess secondary axis formation, the mRNAs were injected into the ventro-vegetal blastomere of 4 cell–stage embryos, and the embryos were then cultured until they reached the larval stage. For explant elongation assay, ectodermal explants from control and treated embryos at the early gastrula stage were dissected and treated with activin (a gift from J.C. Smith). The explants were then cultured until they reached the neurula stage.

RT-PCR

Animal-cap explants from control and treated embryos at the blastula stage were dissected and then cultured until they reached the early gastrula stage. Extraction of RNA, RT-PCR, and primers for *Siamois* and *ODC* were as described (Umbhauer et al., 2000). The RT-PCR results were analyzed by using a phosphoimager system (BioRad).

Supplementary Material

Refer to Web version on PubMed Central for supplementary material.

Acknowledgments

We are grateful to Drs. J.D. Axelrod, W. Birchmeier, D. Ellies, R. Krumlauf, J.I. Morgan, and S.W. White for their critical reading of and valuable comments about the manuscript and to Dr. J.C. Jones for her editing of the manuscript. We thank Dr. W. Zhang for technical support and are grateful for Dr. Xiaoping He for his kind help. This work was supported by the American Lebanese Syrian Associated Charities (to J.Z.), by grants from the National Institutes of Health (to J.Z., D.W., and M.M.), the Centre National de la Recherche Scientifique, the Association Française contre les Myopathies, the Ligue National Contre le Cancer, and the Association pour la Recherche sur le Cancer (to D-.L.S.). D.-L.S. is a Centre National de la Recherche Scientifique investigator.

References

Axelrod JD. Unipolar membrane association of Dishevelled mediates Frizzled planar cell polarity signaling. Genes Dev. 2001; 15:1182–1187. [PubMed: 11358862]

Axelrod JD, Miller JR, Shulman JM, Moon RT, Perrimon N. Differential recruitment of Dishevelled provides signaling specificity in the planar cell polarity and Wingless signaling pathways. Genes Dev. 1998; 12:2610–2622. [PubMed: 9716412]

Bezprozvanny I, Maximov A. Classification of PDZ domains. FEBS Lett. 2001; 509:457–462. [PubMed: 11749973]

Boutros M, Mlodzik M. Dishevelled: at the crossroads of divergent intracellular signaling pathways. Mech Dev. 1999; 83:27–37. [PubMed: 10507837]

Boutros M, Paricio N, Strutt DI, Mlodzik M. Dishevelled activates JNK and discriminates between JNK pathways in planar polarity and wingless signaling. Cell. 1998; 94:109–118. [PubMed: 9674432]

Cadigan KM, Nusse R. Wnt signaling: a common theme in animal development. Genes Dev. 1997; 11:3286–3305. [PubMed: 9407023]

Cheyette BN, Waxman JS, Miller JR, Takemaru K, Sheldahl LC, Khlebtsova N, Fox EP, Earnest T, Moon RT. Dapper, a Dishevelled-associated antagonist of beta-catenin and JNK signaling, is required for notochord formation. Dev Cell. 2002; 2:449–461. [PubMed: 11970895]

Cowburn D. Peptide recognition by PTB and PDZ domains. Curr Opin Struct Biol. 1997; 7:835–838. [PubMed: 9434904]

Daniels DL, Cohen AR, Anderson JM, Brunger AT. Crystal structure of the hCASK PDZ domain reveals the structural basis of class II PDZ domain target recognition. Nat Struct Biol. 1998; 5:317–325. [PubMed: 9546224]

Delaglio F, Grzesiek S, Vuister GW, Zhu G, Pfeifer J, Bax A. NMRPipe: a multidimensional spectral processing system based on UNIX pipes. J Biomol NMR. 1995; 6:277–293. [PubMed: 8520220]

Djiane A, Riou JF, Umbhauer M, Shi DL. Role of frizzled 7 in the regulation of convergent extension movements during gastrulation in Xenopus laevis. Development. 2000; 127:3091–3100. [PubMed: 10862746]

Gloy J, Hikasa H, Sokol SY. Frodo interacts with Dishevelled to transduce Wnt signals. Nat Cell Biol. 2002; 4:351–357. [PubMed: 11941372]

Guntert P, Braun W, Wuthrich K. Efficient computation of three-dimensional protein structures in solution from nuclear magnetic resonance data using the program DIANA and the supporting programs CALIBA, HABAS and GLOMSA. J Mol Biol. 1991; 217:517–530. [PubMed: 1847217]

Guntert P, Mumenthaler C, Wuthrich K. Torsion angle dynamics for NMR structure calculation with the new program DYANA. J Mol Biol. 1997; 273:283–298. [PubMed: 9367762]

Hillier BJ, Christopherson KS, Prehoda KE, Bredt DS, Lim WA. Unexpected modes of PDZ domain scaffolding revealed by structure of nNOS-syntrophin complex. Science. 1999; 284:812–815. [PubMed: 10221915]

Hung AY, Sheng M. PDZ domains: structural modules for protein complex assembly. J Biol Chem. 2002; 277:5699–5702. [PubMed: 11741967]

Krasnow RE, Wong LL, Adler PN. Dishevelled is a component of the frizzled signaling pathway in *Drosophila*. Development. 1995; 121:4095–4102. [PubMed: 8575310]

Li L, Yuan H, Xie W, Mao J, Caruso AM, McMahon A, Sussman DJ, Wu D. Dishevelled proteins lead to two signaling pathways. Regulation of LEF-1 and c-Jun N-terminal kinase in mammalian cells. J Biol Chem. 1999; 274:129–134. [PubMed: 9867820]

Moon RT, Shah K. Developmental biology: signalling polarity. Nature. 2002; 417:239–240. [PubMed: 12015587]

Moon RT, Bowerman B, Boutros M, Perrimon N. The promise and perils of Wnt signaling through beta-catenin. Science. 2002; 296:1644–1646. [PubMed: 12040179]

Noordermeer J, Klingensmith J, Perrimon N, Nusse R. dishevelled and armadillo act in the wingless signalling pathway in *Drosophila*. Nature. 1994; 367:80–83. [PubMed: 7906389]

Nooren IM, Thornton JM. Structural characterisation and functional significance of transient protein-protein interactions. J Mol Biol. 2003; 325:991–1018. [PubMed: 12527304]

Park M, Moon RT. The planar cell-polarity gene stbm regulates cell behaviour and cell fate in vertebrate embryos. Nat Cell Biol. 2002; 4:20–25. [PubMed: 11780127]

Rothbacher U, Laurent MN, Deardorff MA, Klein PS, Cho KW, Fraser SE. Dishevelled phosphorylation, subcellular localization and multimerization regulate its role in early embryogenesis. EMBO J. 2000; 19:1010–1022. [PubMed: 10698942]

Rousset R, Mack JA, Wharton KA Jr, Axelrod JD, Cadigan KM, Fish MP, Nusse R, Scott MP. Naked cuticle targets dishevelled to antagonize Wnt signal transduction. Genes Dev. 2001; 15:658–671. [PubMed: 11274052]

Shulman JM, Perrimon N, Axelrod JD. Frizzled signaling and the developmental control of cell polarity. Trends Genet. 1998; 14:452–458. [PubMed: 9825673]

Siegfried E, Wilder EL, Perrimon N. Components of wingless signalling in *Drosophila*. Nature. 1994; 367:76–80. [PubMed: 8107779]

Sokol SY. Analysis of Dishevelled signalling pathways during Xenopus development. Curr Biol. 1996; 6:1456–1467. [PubMed: 8939601]

Taipale J, Beachy PA. The Hedgehog and Wnt signalling pathways in cancer. Nature. 2001; 411:349–354. [PubMed: 11357142]

Tochio H, Mok YK, Zhang Q, Kan HM, Bredt DS, Zhang M. Formation of nNOS/PSD-95 PDZ dimer requires a preformed beta-finger structure from the nNOS PDZ domain. J Mol Biol. 2000; 303:359–370. [PubMed: 11031113]

Tree DR, Shulman JM, Rousset R, Scott MP, Gubb D, Axelrod JD. Prickle mediates feedback amplification to generate asymmetric planar cell polarity signaling. Cell. 2002; 109:371–381. [PubMed: 12015986]

Umbhauer M, Djiane A, Goisset C, Penzo-Mendez A, Riou JF, Boucaut JC, Shi DL. The C-terminal cytoplasmic Lys-Thr-X-X-X-Trp motif in frizzled receptors mediates Wnt/beta-catenin signalling. EMBO J. 2000; 19:4944–4954. [PubMed: 10990458]

Weston CR, Davis RJ. Signal transduction: signaling specifi. Science. 2001; 292:2439–2440. [PubMed: 11431552]

Wharton KA Jr. Runnin' with the Dvl: proteins that associate with Dsh/Dvl and their significance to Wnt signal transduction. Dev Biol. 2003; 253:1–17. [PubMed: 12490194]

Wong HC, Mao J, Nguyen JT, Srinivas S, Zhang W, Liu B, Li L, Wu D, Zheng J. Structural basis of the recognition of the dishevelled DEP domain in the Wnt signaling pathway. Nat Struct Biol. 2000; 7:1178–1184. [PubMed: 11101902]

Wong HC, Liu G, Zhang YM, Rock CO, Zheng J. The solution structure of acyl carrier protein from Mycobacterium tuberculosis. J Biol Chem. 2002; 277:15874–15880. [PubMed: 11825906]

Wuthrich K. Protein recognition by NMR. Nat Struct Biol. 2000; 7:188–189. [PubMed: 10700272]

Xia, TH.; Bartels, C.; Wuthrich, K. XEASY ETH Automated Spectroscopy for X Window System, User Mannal. ETH-Honggerberg; Zurich: 1993.

Yan D, Wallingford JB, Sun TQ, Nelson AM, Sakanaka C, Reinhard C, Harland RM, Fantl WJ, Williams LT. Cell autonomous regulation of multiple Dishevelled-dependent pathways by mammalian Nkd. Proc Natl Acad Sci USA. 2001; 98:3802–3807. [PubMed: 11274398]

Zheng J, Cahill SM, Lemmon MA, Fushman D, Schlessinger J, Cowburn D. Identification of the binding site for acidic phospholipids on the pH domain of dynamin implications for stimulation of GTPase activity. J Mol Biol. 1996; 255:14–21. [PubMed: 8568861]

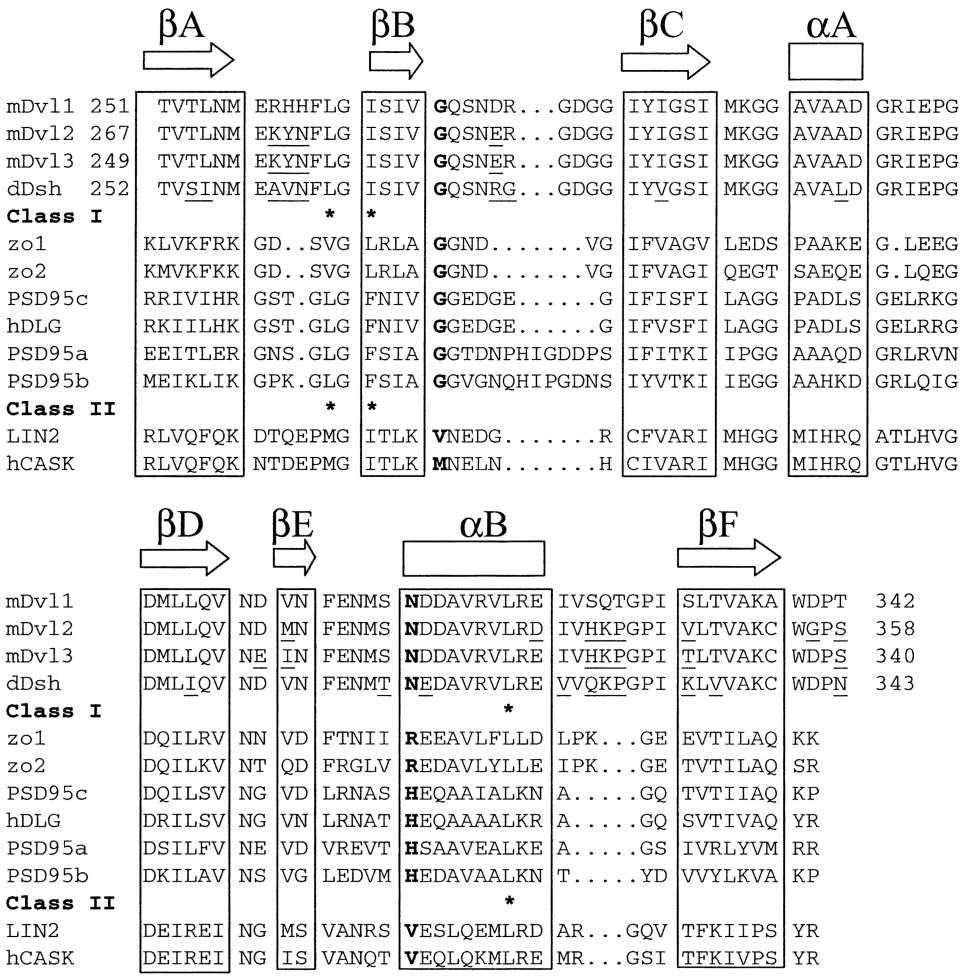

Figure 1. Structure-Based Alignment of the Amino Acid Sequences of the PDZ Domains of Dvl Homologs and Other Proteins

Secondary structural elements are indicated above the sequences. Residues at the GH positions are in boldface type. The asterisk denotes the binding pocket for the ligand's C terminus. Sequence differences among the PDZ domains are indicated by underlining.

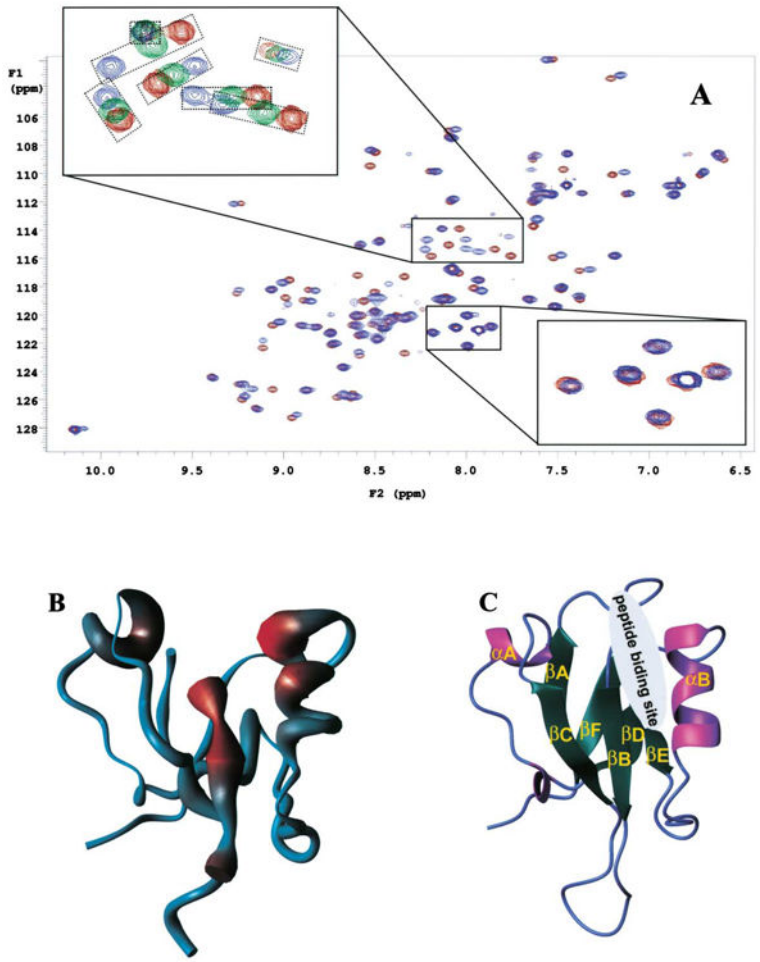

Figure 2. Interaction between the mDvl1 PDZ Domain and Fz7

(A) ^{15}N-HSQC spectra of free Fz7 peptide and Fz7 peptide bound to the PDZ domain of mDvl1. The red contour lines represent spectra of the free form of the PDZ domain when no Fz7 peptide (GKTLQSWRRFYH) was present, the green lines (upper inset) represent spectra of partially bound forms of the PDZ domain when 0.86 mM Fz7 peptide was present, and the blue lines represent spectra of the fully bound forms of the PDZ domain when 10 mM Fz7 peptide was present. The concentration of the PDZ domain was 1.1 mM. The two insets show the enlarged regions where the chemical-shift perturbations were small (lower inset) and large (upper inset). In the upper inset, the signals from the same residue but in different spectra were placed in smaller boxes.

(B) The figure shows the worm representation of the backbone structure of the mDvl1 PDZ domain. The thickness of the worm is proportional to the weighted sum (in Hz) of the ^{1}H and ^{15}N shifts upon binding by the Fz7 peptide (see A), and the increasing chemical-shift perturbation is shown (blue, low; red, high).

(C) Ribbon diagram of the PDZ domain structure. The binding site of the Fz7 peptide identified from the chemical-shift perturbation studies is indicated.

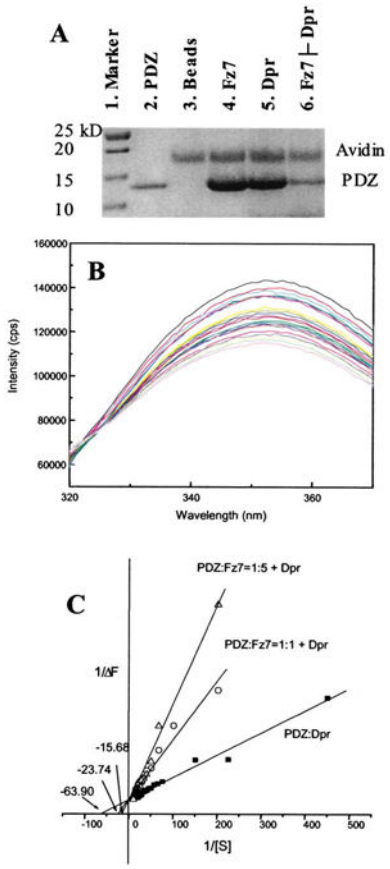

Figure 3. Fz7 and Dpr/Frodo Peptides and Their Binding to the PDZ Domain In Vitro

(A) Biotinylated Fz7 or Dpr/Frodo peptide was coupled to the UltraLink Immobilized Monomeric Avidin, and the avidin-coupled peptides were then incubated with purified PDZ domain. After extensive washing, peptide-interacting proteins were resolved and visualized by SDS-PAGE. Besides those bound to the PDZ domain, some proteins that became detached from the avidin-immobilized beads were also observed. Lane 1, marker. Lane 2, PDZ domain. Lane 3, The PDZ domain and the avidin-agarose beads. Lane 4, The PDZ domain and beads coupled to the Fz7 peptide. Lane 5, the PDZ domain and beads coupled to the Dpr/Frodo peptide. Lane 6: the PDZ domain bound to the Fz7 peptide-coupled beads after elution by the Dpr/Frodo peptide. The experimental condition was similar to that used for the mixture depicted in lane 4, except that before SDS-PAGE, the beads were washed with a buffer that contained Dpr/Frodo peptide.

(B) Fluorescence spectra (labeled with different colors) of the PDZ domain in the presence of various concentrations of Dpr/Frodo peptides. Intrinsic tryptophan fluorescence of the PDZ domain was quenched by bound peptide.

(C) Reciprocal plot of fluorescence data were fitted to a competitive inhibition model in which the Fz7 peptide disrupts the interaction between the Dpr/Frodo peptide and the PDZ domain. Extracted from the fitting, the binding affinity of Dpr/Frodo peptide and the PDZ domain was 16.1 ± 0.7 μM, and the affinity of the Fz7 peptide and the PDZ domain, extracted from the two apparent K_I values at two concentrations (5.9 μM and 12.8 μM, respectively), was 9.5 ± 7.9 μM.

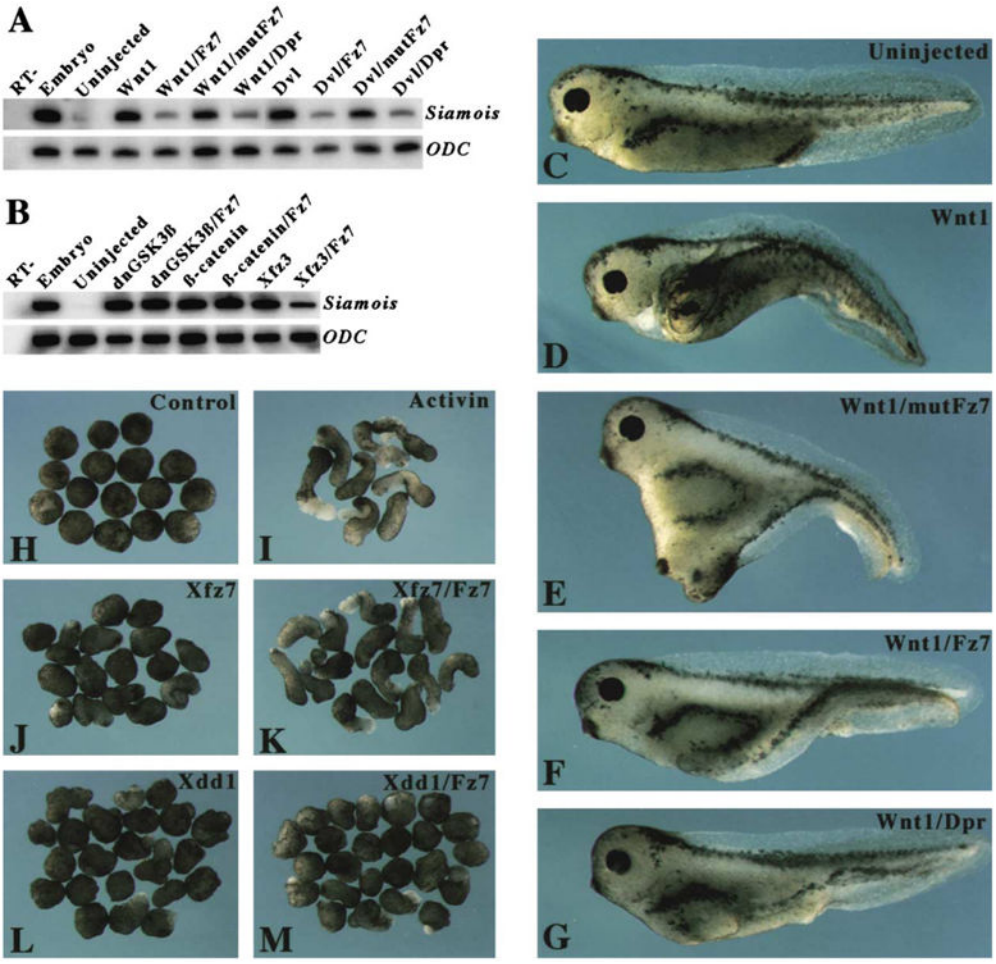

Figure 4. Effects of PDZ Binding Peptides on Canonical Wnt Signaling in *Xenopus* Embryos

(A) The Fz7 and Dpr/Frodo peptides inhibited the canonical Wnt pathway. RT-PCR was conducted to analyze the expression of the *Xenopus* Wnt target gene *Siamois* in ectodermal explants. Synthetic mRNA corresponding to *Wnt1* (1 pg) and *Dvl* (500 ng) were injected alone or were coinjected with PDZ binding peptides (100 ng; corresponding concentration after injection, approximately 200 μM). Injections were administered to the animal-pole region at the 8 cell stage, and ectodermal explants were cultured until they reached the early gastrula stage, at which time they underwent RT-PCR analysis.

(B) The Fz7 peptide had no effect on *Siamois* expression induced by dominant-negative GSK3β (dnGSK3β) or by β-catenin, but it blocked *Siamois* expression induced by Xfz3. RT-, whole-embryo sample analyzed in the absence of reverse transcription. *ODC (ornithine decarboxylase)* was used as a loading control.

(C–G) Blockage of secondary axis formation by PDZ binding peptides. Ventro-vegetal injections of *Wnt1* mRNA (1 pg) and PDZ binding peptides (100 ng; corresponding concentration after injection, approximately 200 μM) were done at the 4 cell stage. Embryos that received injections were cultured until they reached the larval stage; at that point they were analyzed to determine whether any secondary axis was present. (C) A control embryo that received no injection. (D) An embryo that received an injection of *Wnt1* mRNA

developed a complete secondary axis. (E) An embryo that received coinjections of the mutated Fz7 peptide, mutFz7, and *Wnt1* mRNA developed a secondary axis. (F and G) An embryo that received coinjections of *Wnt1* mRNA and either Fz7 (F) or Dpr/Frodo (G) peptide developed a partial secondary axis. (H–M) The Fz7 peptide differentially rescued the effect of Xfz7 and Xdd1 on elongation *of Xenopus* explants. The animal-pole region of embryos at the 4 cell stage received injections of 500 ng synthetic mRNA corresponding to *Xfz7* or *Xdd1* that were given alone or together with the Fz7 peptide. Ectodermal explants dissected at the early blastula stage were treated with activin and cultured until they reached the neurula stage. (H) Untreated explants from control embryos did not show elongation. (I) Activin-treated explants from control embryos exhibited extensive elongation. (J) Xfz7 blocked explant elongation induced by activin. (K) The coinjected Fz7 peptide rescued explant elongation. (L) Xdd1 blocked explant elongation to a similar degree as did Xfz7. (M) The coinjected Fz7 peptide did not rescue explant elongation.

Table 1
Detection of the Fz-Dvl Interaction in a Yeast Two-Hybrid System

Bait: +Gal4-Binding Domain	Prey: +Gal4-Activation Domain	β-Gal Activity (=Blue Colony)
pVA3 (=control)	pTD1 (=control)	+++
Fz_Cterm	pTD1	–
Fz_CtermΔ5	pTD1	–
DFz2_Cterm	pTD1	–
DFz2_CtermΔ5	pTD1	–
pVA3	Dsh (full length as identified in the YTH screen)	
Fz_Cterm	Dsh	++
Fz_CtermΔ5	Dsh	++
DFz2_Cterm	Dsh	++
DFz2_CtermΔ5	Dsh	++
Fz_Cterm	Dsh	++

pVA3, positive control plasmid that encodes a DNA-BD/murine p53 fusion protein. pTD1, positive control plasmid that encodes an AD/SV40 large T antigen fusion protein. Fz, *Drosophila* Frizzled. DFz2, *Drosophila* Frizzled 2. Fz_Cterm, C terminus of *Drosophila* Frizzled. DFz2_Cterm, C terminus of *Drosophila* Frizzled 2. Fz_CtermΔ5, C terminus of *Drosophila* Frizzled with the last five amino acids deleted. DFz2_CtermΔ5, C terminus of *Drosophila* Frizzled 2 with the last five amino acids deleted. Dsh, *Drosophila* Dishevelled.

Table 2

Effects of Fz7 and Dpr/Frodo Peptides on Secondary Axis Formation Induced by Wnt1[a]

Injected material	Complete[b]	Partial[c]	Normal	*n*[d]
Wnt1 (1pg)	51%	44%	5%	117
Wnt1 (1pg)/Fz7 (100 ng)	17%	52%	31%	99
Wnt1 (1pg)/Fz7 (25 ng)	28%	68%	4%	75
Wnt1 (1pg)/mutFz7 (100 ng)	44%	40%	16%	87
Wnt1 (1pg)/Dpr/Frodo (100 ng)	14%	60%	26%	84

[a] Ventro-vegetal injections of *Wnt1* mRNA and the PDZ-binding pep-tides, Fz7 (G**KT**LQS**W**RRFYH), mutFz7 (G**MV**LQS**G**RRFYH), and Dpr/Frodo (SGSLKLMTTV) were done at the4 cell stage. Experimental details are shown in Figures 4C–4G.

[b] Defined as the appearance of a second neural plate on the ventral side of early neurulae and ectopic eyes and cement glands. Percentages indicate the proportion of embryos that met the definition.

[c] Defined as the appearance of an ectopic secondary neural plate that lacked anterior-most structures. Percentages indicate the proportion of embryos that met the definition.

[d] Total number of embryos that received injections in three independent experiments.